Materials Research Proceedings 54 (2025) 87-95 https://doi.org/10.21741/9781644903599-10

Analysis of mechanical and metallurgical properties of HSLA fabricated by wire and arc additive manufacturing (WAAM)

Matheus Miranda[1,a*], Bruno S. Cota[1], Valdemar R. Duarte[2], Tarcísio G. Brito[1], Gustavo H.S.F.L. de Carvalho[3], Telmo G. Santos[2]

[1]UNIFEI - Universidade Federal de Itajubá, Instituto de Engenharias Integradas, Itabira, MG, Brasil

[2]UNIDEMI, Department of Mechanical and Industrial Engineering, NOVA School of Science and Technology, Universidade NOVA de Lisboa, 2829-516, Caparica, Portugal

[3]UNIFI, Università Degli Studi Di Firenze, Dipartimento di Ingegneria Industriale (DIEF), Florence, Italy

[a]matheusfernandesdemiranda@gmail.com

Keywords: Wire Arc Additive Manufacturing, Direct Energy Deposition, Anisotropy, Mechanical

Abstract. A customized WAAM torch was attached to a 3-axis CNC machine within a working envelope of 2760 × 1960 × 2000 mm and a welding machine from Oerlikon, with a power source CITOWAVE III 520, wire feeder and control unit DMU W500 was used to deposit the material over a mild steel substrate. The feedstock material was a commercial low-carbon high-strength steel AWS A5.28 ER110S-G wire electrode with a diameter of 1 mm. ARCAL™ (Ar 82% / CO2 18%) was used as shielding gas and the deposition strategy was the Zig-Zag, i.e. consecutive layers were deposited in opposite directions. The samples were manufactured with 50 layers to carry out mechanical and metallographic tests. Uniaxial tensile tests were performed on an Autograph Shimadzu machine model AG500Kng equipped with a Shimadzu load cell SFL-50kN AG. For each condition, four specimens were removed in the longitudinal direction and four specimens in the transverse direction. The micro-specimens with a thickness of 2.5 mm were extracted via electro discharge machining (EDM), and the geometry was designed on the basis of standards according to the recommendations of ASTM E8-04, DIN EN 2002-001:2006-11 and DIN EN ISO 6892-1:2009-12. Impact tests were performed with a Charpy pendulum (300 J capacity) on V-notch sub-sized samples with dimensions of 55 mm × 10 mm × 2,5 mm according to the specifications given by EN ISO 148–1:2016 [1]. For microstructural characterization, cross-sections from the center of each sample were cut, polished, and etched with Nital (2%). The metallographic analysis was conducted using a Leica DMI 5000 M inverted optical microscope.

Introduction

The Wire and Arc Additive Manufacturing (WAAM) technique combines conventional welding with advanced robotics to fabricate metal parts layer by layer. It is widely applied due to its ability to produce large components, complex geometries, and optimized structures in a cost-effective and efficient manner [2]. However, its industrial implementation requires a detailed understanding of the mechanical behavior of the manufactured materials, necessitating experimental studies on mechanical properties and metallographic characterization [3].

WAAM, classified as a Direct Energy Deposition (DED) process by the ASTM F2792-12a standard, uses a metallic wire as the feedstock, melted layer by layer through an electric arc. This study investigates the impact of layer orientation (vertical and horizontal) on the structural performance of samples fabricated via WAAM, performing tensile tests, Charpy impact tests,

Vickers microhardness measurements, and metallographic analysis to understand the mechanical and structural implications associated with the method.

Literature Review

Applications and Characteristics of the WAAM Method in Additive Manufacturing. The ASTM F2792-12a standard standardizes terminology for additive manufacturing processes, promoting a uniform understanding across various technologies that build parts layer by layer from digital data. The methods are classified into seven main categories:

1. Binder Jetting: A binding agent selectively bonds particles in a powder bed, followed by post-processes like curing or sintering. It is widely used in casting molds and architectural parts production due to its versatility with materials such as metals, sand, and ceramics [4].
2. Directed Energy Deposition (DED): An energy beam, such as a laser, melts and deposits material directly onto the part, making it ideal for repairs and manufacturing complex, high-precision metallic components, especially in aerospace industries [4],
3. Material Extrusion: A heated nozzle deposits polymers or waxes layer by layer. The Fused Deposition Modeling (FDM) technique is popular due to its simplicity and low cost, commonly applied in rapid prototyping [5].
4. Material Jetting: Droplets of photosensitive material are deposited and solidified by UV light, enabling high-quality visual prototypes with varied colors, ideal for design applications [5],
5. Powder Bed Fusion: Techniques like Selective Laser Melting (SLM) and Electron Beam Melting (EBM) use energy beams to fuse metallic or ceramic powder, producing complex parts with high precision and strength, particularly for aerospace and medical industries [4].
6. Sheet Lamination: Thin layers of material are cut and bonded, creating complex structures at reduced costs. It is primarily used for visual prototypes and non-functional parts [5].
7. Vat Photopolymerization: Photosensitive resins are solidified layer by layer using light, such as in SLA (Stereolithography Apparatus) technology, which offers high resolution and detailing, popular in dentistry and jewelry [4].

Wire and Arc Additive Manufacturing (WAAM) is a direct energy deposition technique that combines welding and additive manufacturing, using an electric arc to melt metallic wire. It stands out for its high deposition rate and low cost, being widely applied in the production of large-scale metallic parts [6][7].

Recent Studies. The literature investigates the mechanical behavior of test specimens produced via additive manufacturing using ER110S-G electrodes, focusing on high-strength, low-alloy steel (HSLA). The process involved depositing material on a mild steel substrate, creating 50 layers, each 180 mm long [8].

Table 1 summarizes the tensile test results for horizontal and vertical directions, highlighting yield strength, ultimate tensile strength, and elongation. Additionally, hardness testing revealed a surface hardness of approximately 290 HV, indicating robust surface resistance.

Also observed, through optical microscopy, the presence of ferritic constituents in the analyzed sections. The average hardness of the specimens was below 350 HV, which aligns with expectations for martensite-free HSLA steel with 0.1% carbon contente [8].

Table 1 – Results from tensile tests (adapted)

Yield Strength [MPa]	Ultimate Tensile Strength [MPa]	Elongation [%]
Horizontal: 681 ± 25	Horizontal: 870 ± 37	Horizontal: 39 ± 2.1
Vertical: 707 ± 33	Vertical: 889 ± 16	Vertical: 30 ± 2.8

Materials and methods

Fabrication of the WAAM Part. The equipment used to fabricate the studied part is a customized setup, where a WAAM torch was coupled to a 3-axis CNC machine within a workspace envelope (2760 mm × 1960 mm × 2000 mm). An Oerlikon welding machine with a CITOWAVE III 520 power source, wire feeder, and DMU W500 control unit was used to deposit the material onto a low-carbon steel substrate (350 mm × 60 mm × 8 mm).

The feeding material was a commercial low-carbon, high-strength steel wire electrode AWS A5.28 ER110S-G with a diameter of 1 mm. The chemical composition and mechanical properties of the received wire are shown in Table 2 and Table 3, respectively. ARCAL™ (82% Ar / 18% CO2) was used as a shielding gas, and the deposition strategy was Zig-Zag, where consecutive layers were deposited in opposite directions to avoid height differences between the start and end of the part. The process parameters for producing the sample are presented in Table 4.

Table 2 – Chemical composition of ER110S-G wire (% by weight) [9].

C	Mn	Si	Ni	Cr	Mo	V	Cu
0.08	1.70	0.44	1.35	0.23	0.30	0.08	0.25

Table 3 – Mechanical properties of the material deposited with ER110S-G wire [9].

Yield Strength [MPa]	Tensile Strength [MPa]	Elongation [%]	ISO-V Impact -40ºC [J]	Hardness [HV]
710	790	20	70	295

Table 4 – Process parameters for sample fabrication.

Welding Mode	Number of Layers	Interlayer Temperature	Gas Flow Rate	Wire Feed Rate	Deposition Speed	Working Distance
GMAW	50	200°C	18 l/min	4 m/min	360 mm/min	13 mm

The sample was fabricated with 50 layers for mechanical and metallographic tests, as shown in Fig. 1 . The initial and final 10 mm of the sample were removed to avoid regions with higher susceptibility to defects, and specimens were extracted via electrical discharge machining (EDM).

Figure 1 – Part fabricated by additive manufacturing with 50 layers (Author, 2024).

Preparation of Test Specimens. To conduct destructive tests, a series of detailed steps were followed to ensure accuracy and compliance with technical standards. Initially, micro-samples with a thickness of approximately 5 mm were extracted using electrical discharge machining (EDM) with the EUROSTEC CNC Wire EDM machine, model FW3. Prior to this process, milling was performed using the EUROSTEC FTV-H3I machine to remove surface irregularities from the manufactured part. This milling step was essential for creating a uniform surface, allowing for efficient and precise EDM machining.

The dimensions of the test specimens were carefully selected in accordance with current standards for destructive tests, while considering the limitations related to extracting the specimens from the additive-manufactured part. For meaningful results, the extraction process followed the criteria outlined in Fig. 2.

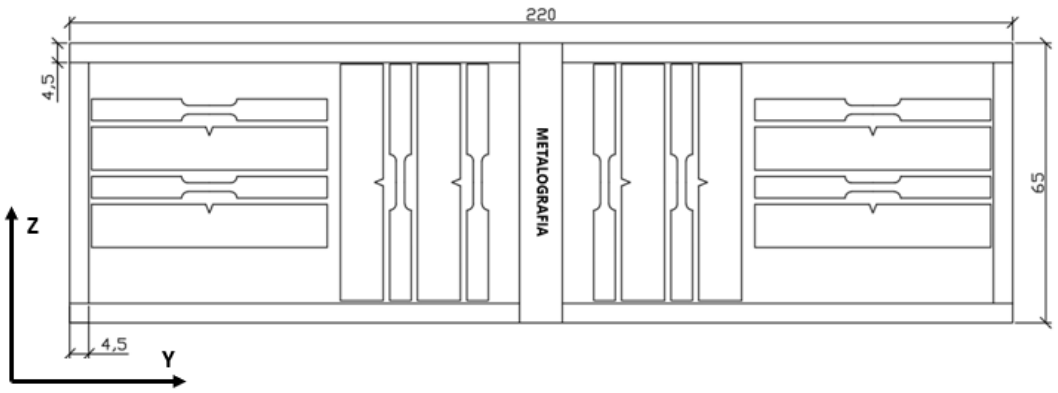

Figure 2 – Extraction Scheme for Test Specimens (all dimensions in mm) (Author, 2024).

Charpy Impact Test. Impact tests were conducted using a Charpy pendulum machine (300 J capacity) on sub-size samples with a V-notch and dimensions of 55 mm × 10 mm (L × W) as per ASTM E23 specifications. As shown in Fig. 2, four samples were extracted in the longitudinal direction and four in the transverse direction for tests conducted at room temperature.

The Charpy impact test was carried out at the facilities of the Nuclear Technology Development Center (CDTN) using a conventional impact testing machine, Wolpert brand, model PW30. The machine has a maximum capacity of 30 kg·m (~300 J), making it suitable for evaluating high-impact-resistant materials.

In accordance with ASTM E23-18, when sub-size specimens are used instead of full-size ones, a normalization factor must be applied to adjust the results, enabling proper comparison between different samples. The normalization factor is based on the ratio of the cross-sectional areas of the test specimens.

Tensile Test. Uniaxial tensile tests were conducted using an MC WDW-100E machine equipped with a 100 kN load cell. A crosshead speed of 0.017 mm/s was established, and tests were performed at room temperature. Test specimens were extracted in both the longitudinal and transverse directions, with four samples in each direction as per the scheme shown in Fig. 2. The sample geometry was designed based on the recommendations of ASTM E8.

The anisotropy of tensile strength and elongation was calculated based on the tensile test data using Eq. 1, where AAA represents the percentage of anisotropy, PmaxP_{max}Pmax is the maximum value among the average horizontal or vertical results, and PminP_{min}Pmin is the minimum [10].

$$A = \frac{P_{max} - P_{min}}{P_{max}} \cdot 100. \quad (1)$$

Metallographic Examination. For metallographic analysis of the part produced via Wire Arc Additive Manufacturing (WAAM), the sample was prepared following a sequence of steps to ensure high-quality results. Initially, the part was sectioned into appropriately sized samples for analysis using a precision cutting machine, ensuring uniform surfaces suitable for subsequent metallographic preparation stages. These procedures followed ASTM E3:2023 standards for sample preparation and ASTM E407:2023 standards for chemical etching of metals and alloys.

The samples were then embedded in phenolic resin (bakelite) using the EM30D HD metallographic embedding machine. This step was crucial for handling the samples during grinding and polishing while preventing damage to sample edges. After embedding, sequential grinding was performed with silicon carbide sandpapers, starting with 120 grit and advancing to 2500 grit. This process was conducted on a PLC grinder and polisher (Fortel brand) with constant lubrication to progressively reduce surface irregularities and prepare the sample for polishing.

Polishing was performed using alumina abrasive material on an automatic polisher to eliminate sanding marks and provide a low-roughness surface, critical for observing microstructural details.

After polishing, the microstructure of the part was revealed via chemical etching with 2% Nital, composed of 2% nitric acid (v/v) and 98% ethanol (v/v). The etching time was carefully controlled to avoid excessive corrosion while adequately highlighting different phases and structures of the alloy without compromising the sample's integrity.

Microscopic analysis was carried out using an OPTON trinocular metallographic microscope. Various sample regions were observed and documented, with images captured at magnifications of 200x and 400x to allow a detailed interpretation of the microstructural characteristics resulting from the WAAM process. These procedures ensured precise microstructural data essential for analyzing and understanding the structural properties and characteristics of the additively manufactured material.

Microhardness Testing. The Vickers hardness test was conducted to evaluate the hardness distribution along the height of the part manufactured by the WAAM method. A Wilson Instruments 402MVD device was used for the test, following ISO 6507:2018 standards. The same specimen used for metallographic analysis was employed for the hardness test.

Hardness measurements were taken along a line perpendicular to the longitudinal axis of the part at regular 1 mm intervals, starting from the substrate base and proceeding to the top of the piece. This approach mapped potential variations in mechanical properties across the solidification gradient characteristic of the WAAM process. A load of 200 gf was applied for 10 seconds.

Results and discussion

Charpy Impact Test. The results of the Charpy impact test on the additive-manufactured samples, oriented horizontally and vertically, are presented in Table 5 and Fig. 3. These results include the normalization factor for the cross-sectional area of each specimen and demonstrate significant differences in absorbed energy based on sample orientation.

Table 5 – Charpy Impact Test Results (Author, 2024).

Sample	Orientation	Absorbed Energy [J]
1	Transverse	80.7
2	Transverse	79.6
3	Transverse	64.9
4	Transverse	69.1
Average	Transverse	73.6 ± 6.7
5	Longitudinal	89.1
6	Longitudinal	81.0
7	Longitudinal	112.4
8	Longitudinal	105.7
Average	Longitudinal	97.1 ± 12.5

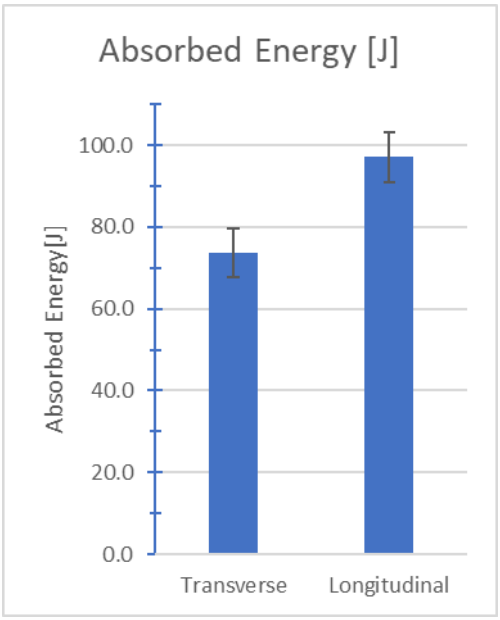

Figure 3 – Charpy impact test results (Author, 2024).

Longitudinal samples (y) absorbed an average of 97.1 J ± 12.5 J, while transverse samples (z), aligned with the weld passes, absorbed 73.6 J ± 6.7 J, a difference of 31.9%. This indicates that the orientation relative to the welding pass significantly impacts impact toughness.

Transverse samples showed greater susceptibility to crack propagation along deposited layers, reducing impact resistance. In contrast, longitudinal samples, where the impact is perpendicular to the weld passes, dissipated more energy before fracturing, as the layer alignment acts as a natural barrier against crack propagation, enhancing material toughness.

Tensile Test.The tensile test results for the additive-manufactured samples are shown in Table 6 and Fig. 4, allowing for detailed analysis of mechanical properties such as yield strength, tensile strength, elongation, and elastic modulus.

Table 6 – Tensile Test Results (Author, 2024).

Sample	Orientation	Yield Strength [MPa]	Tensile Strength [MPa]	Elongation [%]	Elastic Modulus [GPa]
1	Transverse	554.39	769.59	15.7	11.14
2	Transverse	544.71	761.21	18.7	11.29
3	Transverse	526.31	743.87	15.3	10.83
4	Transverse	552.06	818.71	16.7	11.67
Average	Transverse	544.37 ± 11.02	773.35 ± 22.79	16.53 ± 1.2	11.23 ± 0.30
5	Longitudinal	622.73	877.27	17.9	9.69
6	Longitudinal	599.77	823.00	17.8	8.99
7	Longitudinal	474.06	767.04	18.0	11.94
8	Longitudinal	449.76	741.63	16.8	8.96
Average	Longitudinal	536.58 ± 75.60	802.24 ± 52.38	17.63 ± 0.5	9.90 ± 1.22

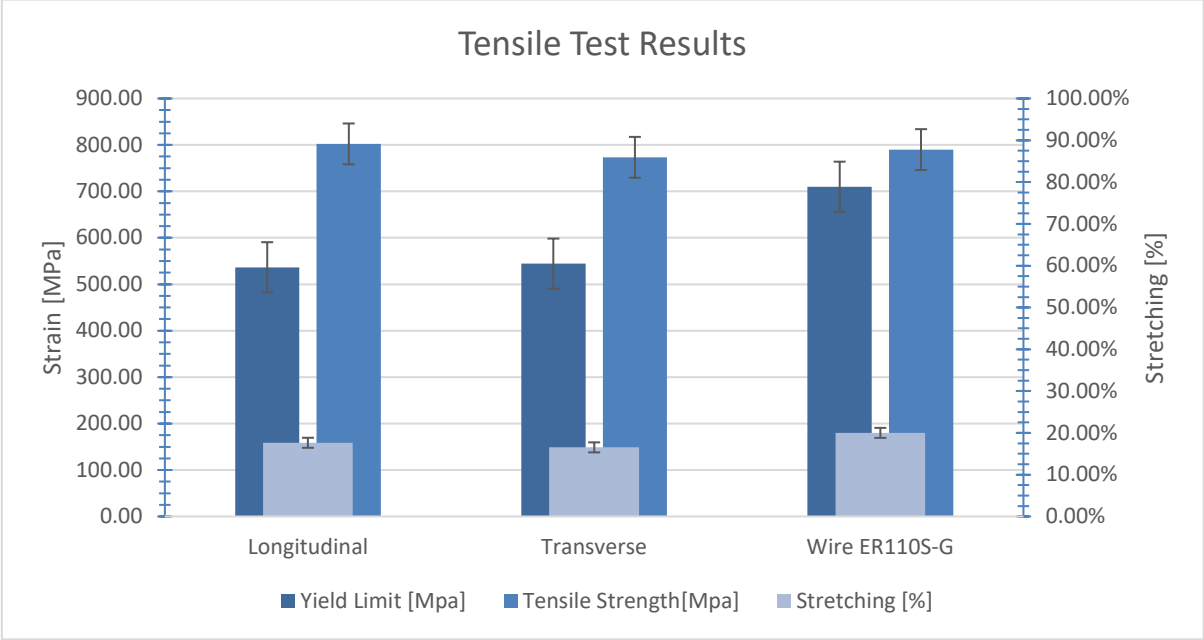

Figure 4 – Tensile test results (Author, 2024).

Transverse samples exhibited an average elastic modulus of 11.23 GPa ± 0.30 GPa, 13.43% higher than the longitudinal (9.90 GPa ± 1.22 GPa), indicating greater rigidity due to layer orientation relative to the applied load.

The average tensile strength was 773.35 MPa ± 22.79 MPa for transverse samples and 802.24 MPa ± 52.38 MPa for longitudinal samples, showing slight superiority in the longitudinal direction due to better load distribution across layers.

The yield strength was similar between orientations: 544.37 MPa ± 11.02 MPa (transverse) and 536.58 MPa ± 75.60 MPa (longitudinal), with a slight advantage for transverse samples, potentially benefiting applications requiring higher resistance to initial plastic deformation.

Metallographic Analysis. The metallographic results identified microconstituents such as acicular ferrite (AF), second-phase ferrite (FS) in aligned (A) and unaligned (NA) forms, dendrites (D), and grain boundary ferrite (GF). These structures are associated with solidification and thermal conditions during the WAAM process and influence the mechanical and metallurgical properties.

Acicular ferrite forms at moderate cooling rates, enhancing mechanical strength and toughness. Aligned ferrite results from thermal gradients, while unaligned ferrite forms under isotropic cooling, contributing to anisotropic material properties [11].

Dendrites and grain boundary ferrites affect segregation and crack resistance, with their morphology influenced by cooling rates and chemical composition [12].

Vickers Microhardness Test. The Vickers hardness profile of the WAAM-manufactured part was analyzed, with results shown in Fig. 5. The hardness averaged 316.5 HV, with variations along the section due to thermal effects during deposition.

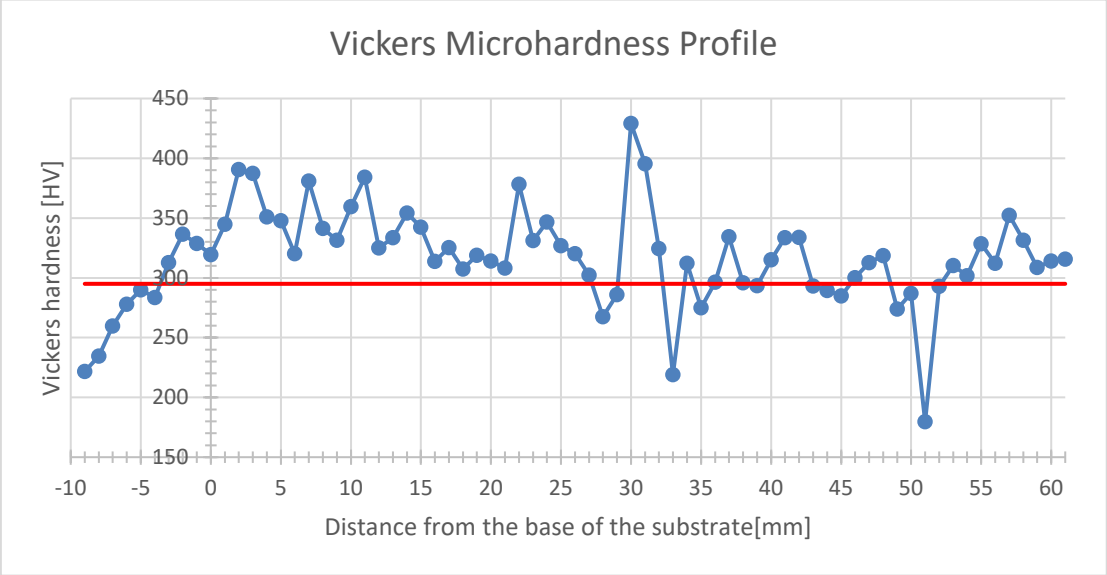

Figure 5 – Vickers microhardness profile along the cross-section (Author, 2024).

Hardness was highest at the base, attributed to greater heat input and refined microstructure in the initial layers. Variations toward the top reflect process parameters and interlayer fusion.

Conclusion

The increasing diffusion of additive manufacturing, especially the WAAM (Wire Arc Additive Manufacturing) method, underscores the importance of understanding the properties and limitations of the materials used in this process. The results obtained allowed for the identification and analysis of the anisotropic properties of the specimens fabricated with ER110S-G wire. Through destructive testing, it was possible to evaluate the material's performance in different deposition orientations.

The results demonstrated an anisotropy of 15.46% for maximum tensile strength and 16.85% for elongation, reflecting the expected behavior of materials produced by additive manufacturing. These variations are associated with the layer-by-layer deposition and the preferential grain orientation during solidification, which are intrinsic characteristics of the WAAM process. Despite the presence of anisotropy, the values obtained fall within the expected range for this manufacturing method, demonstrating its feasibility for industrial applications requiring high-performance metal parts.

Vickers hardness tests indicated variation along the height of the piece, with average values higher than those of the base ER110S-G wire used in the process. Greater hardness was observed at the base of the piece, attributed to the higher heat input during the initial layers, which resulted in a finer microstructure. This variation along the solidification gradient highlights the influence of thermal cycles on the distribution of mechanical properties.

The metallographic analysis revealed predominantly ferritic microstructures, including acicular ferrite, second-phase ferrite (aligned and unaligned), grain boundary ferrites, and dendrites. These characteristics are directly associated with the cooling and deposition conditions of the WAAM method. The identified microstructures contribute to a balance between mechanical strength and ductility.

Charpy impact tests indicated significant differences between the longitudinal and transverse directions, highlighting the influence of orientation on the material's energy absorption capacity. This difference suggests that deposition orientation is a critical factor in defining impact toughness, reinforcing the importance of optimizing manufacturing parameters to meet the specific requirements of each application.

References

[1] T.A. Rodrigues, V. Duarte, J.A. Avila, T.G. Santos, R.M. Miranda, J.P. Oliveira, Wire and arc additive manufacturing of HSLA steel: Effect of thermal cycles on microstructure and mechanical properties, Addit. Manuf. 27 (2019) 440–450. https://doi.org/10.1016/j.addma.2019.03.029

[2] GARDNER, L. Metal additive manufacturing in structural engineering: review, advances, opportunities and outlook. *Structures*, 2023. https://doi.org/10.1016/j.istruc.2022.12.039

[3] GARDNER, L.; KYVELOU, P.; HERBERT, G.; BUCHANAN, C. Testing and initial verification of the world's first metal 3D printed bridge. *Journal of Constructional Steel Research*, 2020. https://doi.org/10.1016/j.jcsr.2020.106233

[4] GIBSON, Ian; ROSEN, David; STUCKER, Brent. Additive Manufacturing Technologies: Rapid Prototyping to Direct Digital Manufacturing. 2. ed. New York: Springer, 2015. https://doi.org/10.1007/978-1-4939-2113-3

[5] GEBHARDT, Andreas. Handbook of Additive Manufacturing. München: Carl Hanser Verlag, 2016.

[6] MARTINA, F. et al. Cold rolling techniques in WAAM. *Materials*, 2019.

[7] RODRIGUES, T. A.; et al. Current Status and Perspectives on Wire and Arc Additive Manufacturing (WAAM). *Materials*, 2019. https://doi.org/10.3390/ma12071121

[8] RODRIGUES, T. A.; DUARTE, V. R.; TOMÁS, D.; et al. In-situ strengthening of a high strength low alloy steel during Wire and Arc Additive Manufacturing (WAAM). *Additive Manufacturing*, 2020. https://doi.org/10.1016/j.addma.2020.101200

[9] LINCOLN ELECTRIC. *Technical Data of ER110S-G Consumable Wire*. 2016. Disponível em: https://www.lincolnelectric.com/assets/global/Products/ConsumableEU_MIGWires-LNM-LNMMoNiVa/lnmmoniva-eng.pdf

[10] KOK, Y.; TAN, X. P. P.; WANG, P.; NAI, M. L. S. L. S.; LOH, N. H. H.; LIU, E.; et al. Anisotropy and heterogeneity of microstructure and mechanical properties in metal additive manufacturing: a critical review. *Materials and Design*, 2018. https://doi.org/10.1016/j.matdes.2017.11.021

[11] ABBASCHIAN, Reza; REED-HILL, Robert E.; ABBASCHIAN, Lara. *Physical Metallurgy Principles*. 4. ed. Stamford: Cengage Learning, 2010.

[12] FLEMINGS, Merton C. Solidification Processing. New York: McGraw-Hill, 1974.

GARCIA, Amauri; SPIM, Jaime A.; SANTOS, Carlos A. *Ensaios de Materiais*. 2. ed. Rio de Janeiro: LTC, 2012.